Localization of a Proton-Pumping ATPase in Rat Kidney

Dennis Brown,* Sheldon Hirsch,‡ and Stephen Gluck‡§
*The Renal Unit and Department of Pathology, Harvard Medical School, Massachusetts General Hospital, Boston, Massachusetts 02114; and ‡Departments of Medicine, and §Cell Biology and Physiology, Washington University School of Medicine, and The Renal Division, Jewish Hospital, St. Louis, Missouri 63110

Abstract

The distribution of vacuolar H^+ATPase in rat kidney was examined by immunocytochemistry using affinity-purified antibodies against the 31-, 56-, and 70-kD subunits of the bovine kidney proton pump. Proximal convoluted tubules were labeled over apical plasma membrane invaginations, and in the initial part of the thin descending limb, apical and basolateral plasma membranes were moderately stained. Thick ascending limbs and distal convoluted tubules were apically stained although the intensity was greater in the distal convoluted tubule. Collecting duct principal cells were virtually unlabeled, but intercalated cells had intense staining with an apical, basolateral or diffuse pattern in the cortex, and exclusively apical staining in the medulla. These results (*a*) show the presence of an H^+ATPase in the apical plasma membrane of the proximal tubule that may contribute to H^+ transport in this segment; (*b*) provide direct evidence that the intercalated cell contains most of the H^+ATPase detectable in the collecting duct, supporting its proposed role in H^+ transport; (*c*) demonstrate that subpopulations of cortical intercalated cells have opposite polarities of an H^+ATPase, consistent with the presence of both proton- and bicarbonate-secreting cells; and (*d*) suggest a role for the H^+ATPase in acid/base regulation or H^+ transport in segments other than the collecting duct and the proximal tubule.

Introduction

The kidney plays a vital role in acid-base homeostasis, by reabsorbing filtered bicarbonate and regenerating bicarbonate consumed by metabolism. These processes are accomplished by renal H^+ secretion, which occurs primarily in the proximal tubule and the collecting duct. Physiological studies have established that Na-H exchange accounts for much of the proximal tubule acidification (1), whereas in more distal segments, acidification is carried out by an electrogenic proton pump thought to be located primarily in the cell type specialized for proton transport, the intercalated cell (2–9). Recent studies have suggested a possible role for a proton pump in proximal tubule acidification (8, 10–13) as well as in the function of other nephron segments, but a definitive demonstration of H^+ATPase involvement in these segments has not been possible because of the lack of a specific inhibitor of the enzyme. An independent method for examining the potential role of an enzyme in nephron function is to localize it with antibody probes. Towards this end, we recently isolated a vacuolar H^+ATPase from bovine kidney medulla and cortex (14–16). The enzyme is a large molecular weight protein with multiple subunits. Since physiologically similar proton pumps have been described in a variety of intracellular membrane compartments (17), the role of this protein in renal hydrogen ion transport has remained unresolved. In this report, we describe the use of polyclonal antibodies specific for each of three subunits of the isolated kidney enzyme to map the distribution of the H^+ATPase in the kidney. The results show that this vacuolar-type enzyme is on the plasma membrane of intercalated cells, where it probably functions as the proton pump responsible for distal acidification. The H^+ATPase is also located on the plasma membranes of epithelial cells from the proximal tubule and some other nephron segments, where it may function in epithelial H^+ transport or cell pH regulation.

Methods

Preparation of antibodies

H^+ATPase was affinity purified from solubilized bovine kidney medulla membranes on a column to which a monoclonal antibody against a bovine medullary H^+ATPase had been covalently coupled (15). The preparation of the monoclonal antibody and its use in affinity purification of the enzyme are described in detail elsewhere (15, 18). The eluate from the affinity column was used to raise polyclonal antisera in rabbits, as previously described (2). Briefly, a 1-mg/ml solution of H^+ATPase was coupled to keyhole limpet hemocyanin with 1-ethyl-3-(3-dimethylaminopropyl)-carbodiimide, and the coupled protein was mixed with complete Freund's adjuvant. New Zealand white rabbits were immunized by intradermal injection, and were boosted after 1 mo, and at 3-wk intervals thereafter. Serum from animals was taken after 6–9 mo of immunization, and was screened by immunoblotting.

To prepare antibodies against specific enzyme subunits, the subunits were separated by SDS-PAGE and transferred to nitrocellulose filters. Strips of filters containing individual subunits were cut from the nitrocellulose and used to absorb subunit-specific IgGs from the holopolyclonal serum, as previously described (2, 19). Antibodies against the 31-, 56-, and 70-kD subunits of the enzyme were prepared in this way, and their subunit specificity was shown by immunoblotting (Fig. 1).

Tissue preparation

Adult Sprague-Dawley rats were anesthetized with Inactin and their kidneys perfused via the left ventricle first with HBSS for 1–2 min, then with a fixative containing 2% paraformaldehyde, 10 mM sodium periodate, and 75 mM lysine (20) for 10 min. Kidneys were removed and immersed overnight in the same fixative at 4°C. For light microscopy, pieces of kidney from different kidney regions were separated and embedded in LX-112 resin (Ladd Industries, Burlington, VT) without postfixation in osmium. For electron microscopy, smaller pieces were

Address reprint requests to Dr. Brown, The Renal Unit, MGH-East, 149 13th Street, Charlestown, MA 02129.

Received for publication 11 February 1988 and in revised form 14 July 1988.

J. Clin. Invest.

0021-9738/88/12/2114/13 $2.00
Volume 82, December 1988, 2114–2126

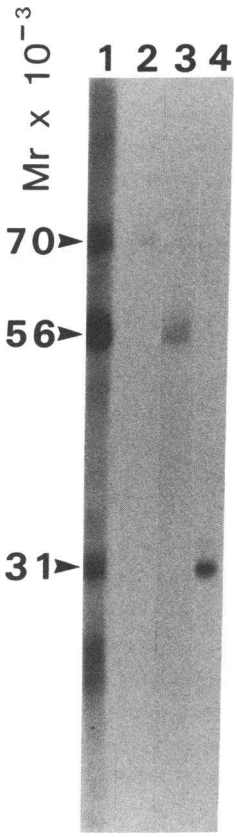

Figure 1. Immunoblot to show the specificity of the antibodies against the H^+ATPase subunits. The unpurified holoantiserum (lane *1*) recognized several bands from kidney microsomal membranes, whereas the affinity-purified antibodies were subunit specific (lanes *2, 4*).

dehydrated in dimethylformamide and embedded in Lowicryl K4M according to a rapid embedding protocol (21).

Immunocytochemistry

Light microscopy. Semithin (1 μm) sections were cut from tissue embedded in LX-112 and were treated for 2 min with a mixture of 2 g KOH, 5 ml propylene oxide, and 10 ml methanol to remove the resin (22). Sections were incubated for 10 min in PBS (0.9% NaCl in 10 mM sodium phosphate buffer, pH 7.4) containing 1% BSA to reduce nonspecific background staining, followed by a 2-h incubation at room temperature with a 20-μl drop of undiluted specific anti-H^+ATPase subunit antibody. After 3 × 5-min rinses in PBS, sections were incubated for 1 h with goat anti-rabbit IgG coupled to fluorescein isothiocyanate (Calbiochem-Behring Corp., San Diego, CA), diluted 1:30, for detection of antigenic sites by immunofluorescence microscopy. Sections were then rinsed 3 × 5 min in PBS and mounted in Gelvatol containing 4% *n*-propyl gallate (Sigma Chemical Co., St. Louis, MO) to retard quenching of the fluorescence (23). Photographs of sections were taken on Kodak Tri-X Pan film using an Olympus BHS photomicroscope with epifluorescence. Some sections were also incubated using the ABC-peroxidase procedure. After incubation with the primary IgG, a biotinylated goat anti-rabbit IgG (Vector Laboratories, Burlinghame, CA) was applied to sections for 1 h, followed by the ABC reagent (also from Vector Laboratories) for a further 1 h. Peroxidase was revealed with diaminobenzidine and H_2O_2, and the sections were dehydrated in ethanol and mounted in Permount (Fisher Scientific Co., Fair Lawn, NJ).

Electron microscopy. Thin sections picked up on nickel grids were processed with no prior etching procedure. Sections were incubated for 10 min on a drop of PBS, followed by 10 min on a drop of PBS containing 1% BSA, to reduce background staining. The sections were transferred to 10-μl drops of undiluted affinity purified antibody against defined subunits of the H^+ATPase, and incubated for 2 h at room temperature in a moist chamber. Sections were then rinsed 3 × 5 min by floating on drops of PBS, and transferred to 20-μl drops of a 1:70 dilution of protein A-gold solution in PBS/1% BSA. The gold was prepared by adsorbing 120 μg protein A (Pharmacia Fine Chemicals, Uppsala, Sweden) to 20 ml of 8 nm colloidal gold suspension (24), and the pellet formed after centrifugation at 60,000 *g* for 45 min was resuspended in 2.0 ml PBS containing 0.2 mg/ml PEG (20,000 mol wt). After 1 h at room temperature, sections were washed 2 × 5 min with PBS and for 5 min on a drop of distilled water. The sections were stained for 7 min with 2% aqueous uranyl acetate and 1 min with lead citrate, and were examined and photographed on a Jeol 1200-EX electron microscope.

Quantification of labeling

The intensity of gold particle labeling was quantified in different segments of the urinary tubule. 10 cells were examined from each region. The labeling over plasma membranes was counted, as well as the labeling of the intracellular H^+ATPase-lined vesicles in intercalated cells. Photographs of apical and basolateral plasma membranes were printed at a final magnification of 45,000 for counting, and the number of gold particles per micrometer length of membrane domain was measured using a graphics tablet and Sigmascan software (Jandel Scientific, Sausalito, CA) connected to an IBM PS2 model 50 computer. Data were stored and analyzed using the Quattro spreadsheet (Borland, Scotts Valley, CA).

Results

For simplicity, we describe the labeling patterns observed by light and electron microscopy in each segment of the urinary tubule in a sequential manner, beginning with the proximal tubule. Antibodies to the 70-, 56-, and 31-kD subunits of the kidney H^+ATPase all gave similar qualitative staining patterns. By electron microscopy, labeling with all three antibodies was seen on the cytoplasmic face of plasmalemmal and intracellular membranes. Control incubations using either normal rabbit serum or antibodies preincubated with purified H^+ATPase gave no detectable staining.

Glomerulus. No specific staining was detectable in the glomerulus.

Proximal tubule. A low power view of the labeling pattern seen in the cortex is shown in Fig. 2. Epithelial cells of the proximal convoluted tubule showed a marked fluorescent staining at the base of the brush border (Figs. 2–4). In the S1 segments, the brush border itself was also faintly stained, but other intracellular structures (such as lysosomes) were not specifically stained. The autofluorescence of the lysosomes in some sections makes low levels of specific fluorescent labeling difficult to detect, but lysosomes also appeared unstained using immunoperoxidase labeling procedures (not shown). By electron microscopy, the bulk of the gold particle labeling was seen overlying apical invaginations, and a smaller amount was associated with the membranes of microvilli (Fig. 5). The labeled invaginations appeared distinct from the coated pits previously shown to be labeled with anti-clathrin antibodies (25, 26). The clathrin-coated membranes were apparent in K4M-embedded tissues even in the absence of specific immunolabeling, because they have a distinct, clear halo on their cytoplasmic side (see Fig. 5). The invaginations that are labeled with anti-H^+ATPase antibodies do not have this halo and were not labeled with anti-clathrin antibodies in a previous report (25). Nevertheless, a double label study at the ultrastructural level will be required to establish definitively whether these clathrin-coated membrane domains exclude H^+ATPase immunoreactive sites.

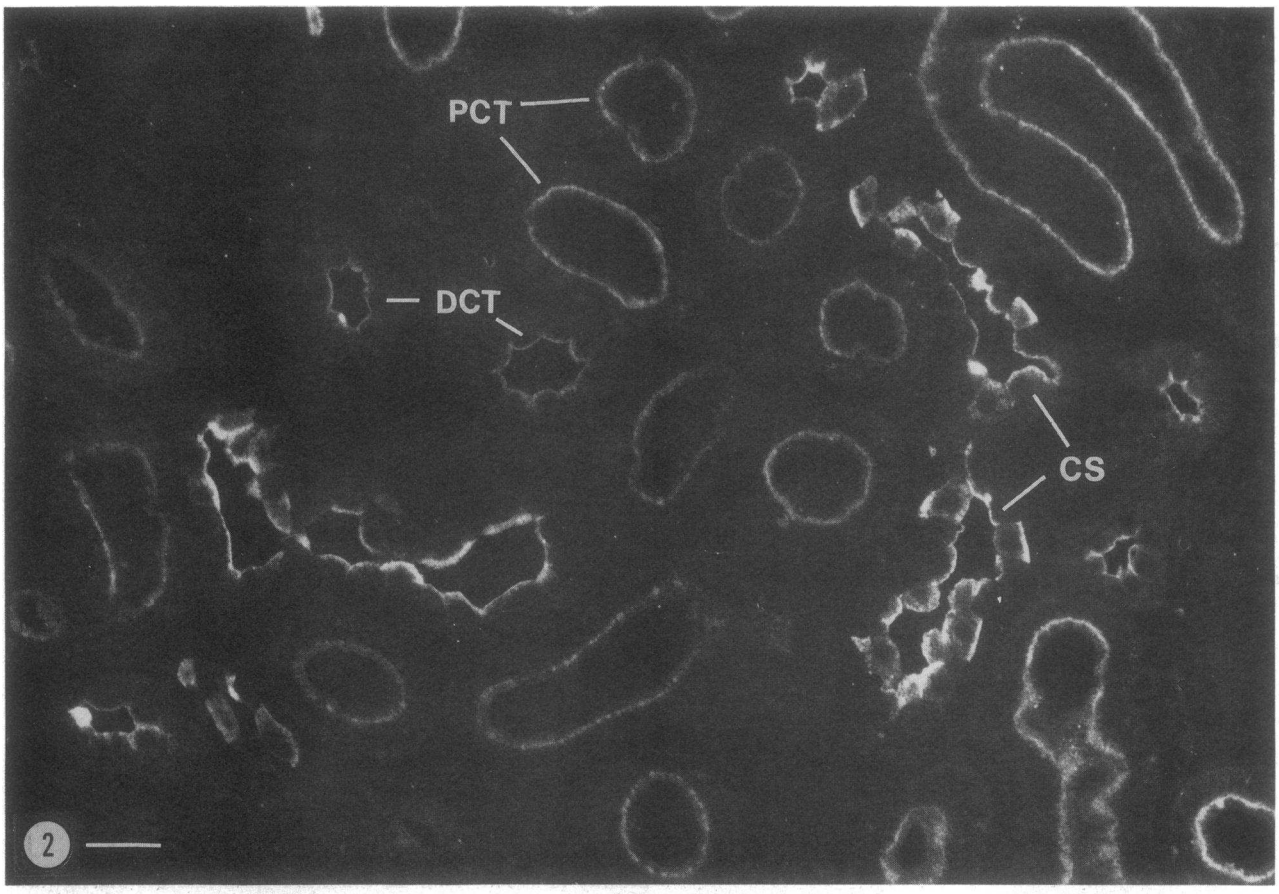
PCT
DCT
CS
2

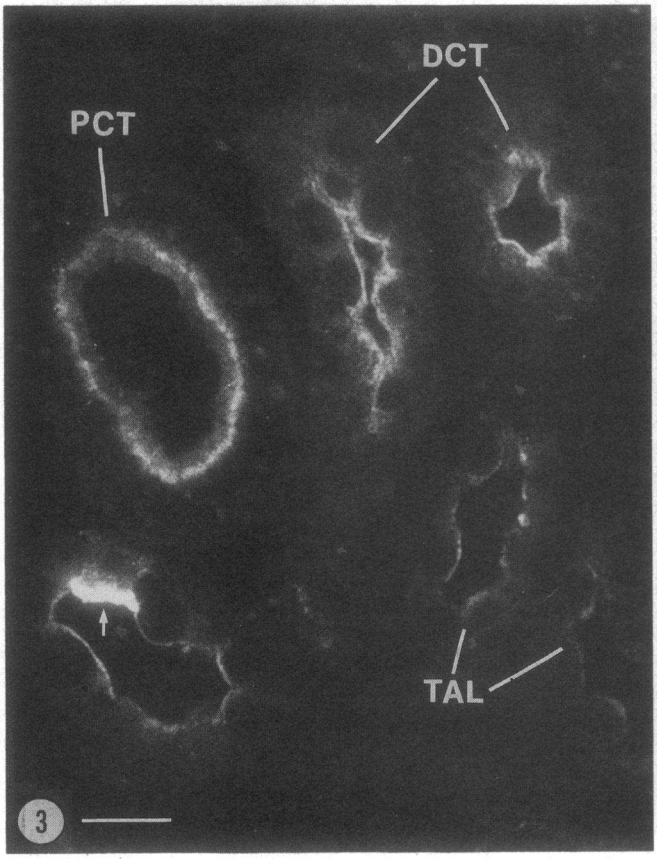
DCT
PCT
TAL
3

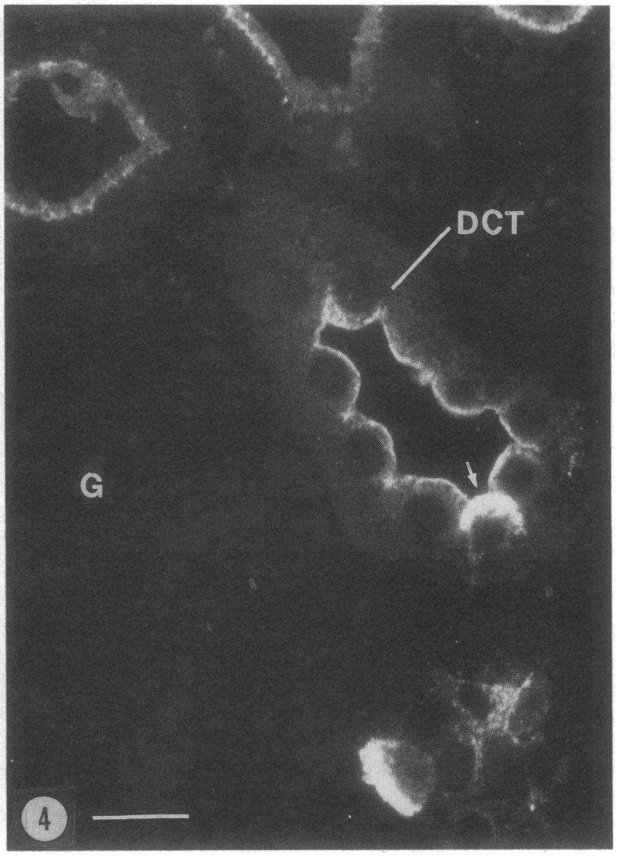
DCT
G
4

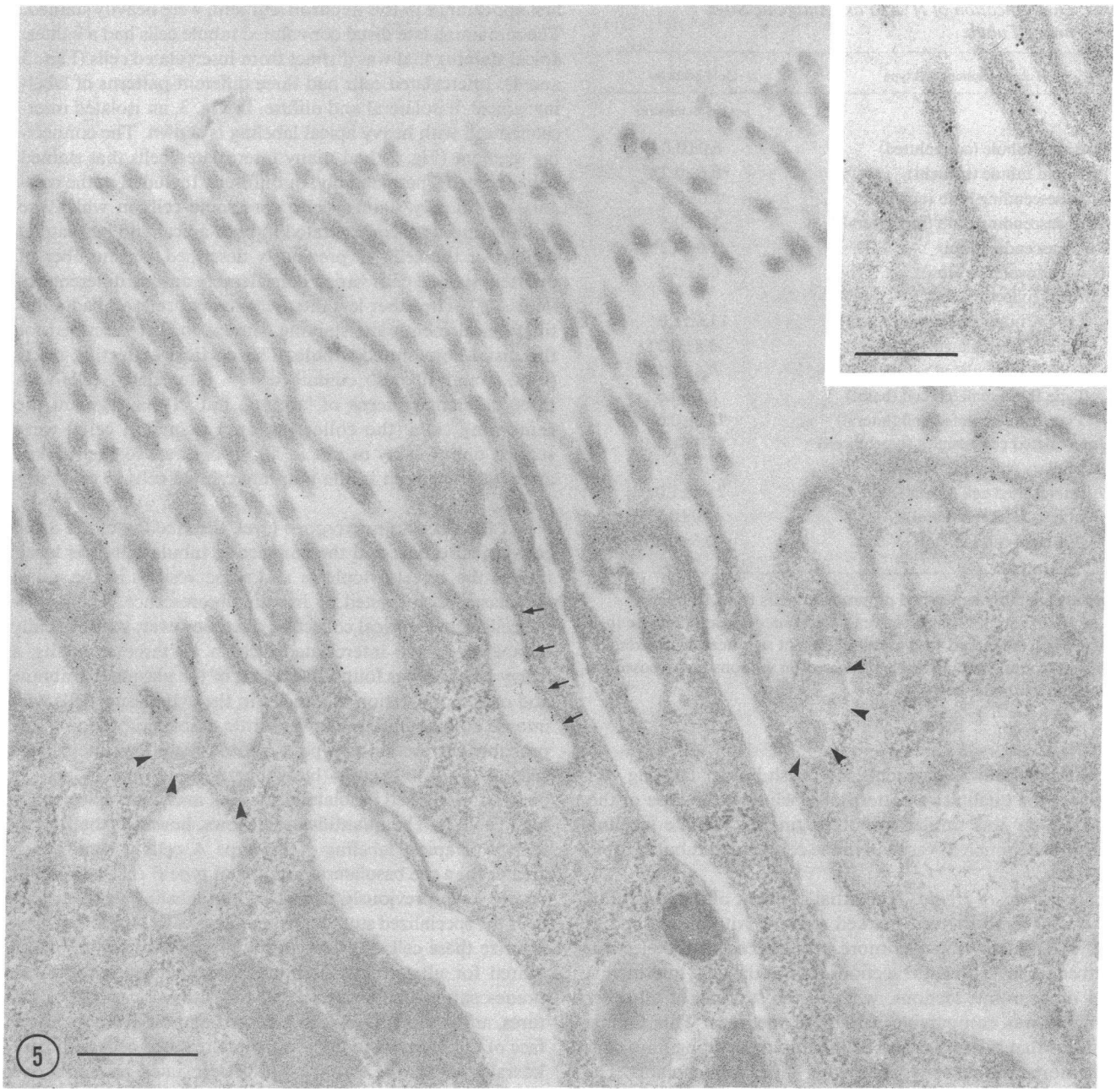

Figure 5. Electron micrograph of the apical part of a cell from the proximal convoluted tubule. The tissue was embedded in Lowicryl K4M and incubated with the anti-56-kD subunit antibody, followed by a further incubation with protein A-gold. Antigenic sites, revealed by the 8-nm gold particles, are concentrated over the plasma membrane at the base of the microvilli (*arrows*), and are much less abundant over the rest of the microvilli. Membrane segments that have a clear halo on their cytoplasmic side appear virtually unlabeled (*arrowheads*). These regions probably correspond to the clathrin-coated invaginations and vesicles previously detected by immunocytochemistry in the proximal tubule (25, 26). The inset shows part of the apical region of a labeled proximal convoluted tubule cell at higher magnification. Bar = 0.5 μm (*inset*, Bar = 0.25 μm).

Figures 2–4. Semithin sections of rat kidney cortex incubated with antibody against the 31-kD subunit of H^+ATPase, followed by goat anti-rabbit IgG coupled to FITC. (*Fig. 2*) Low power view of the cortex, showing staining of different nephron segments. Proximal convoluted tubules (PCT) have a band of labeling at the base of the brush border. The epithelial cells of the distal convoluted tubule (DCT) are all labeled at their apical pole. In the connecting segment (CS), a complex pattern of labeling is seen. Intercalated cells are heavily labeled at either the apical or basal pole, or have a more diffuse labeling that is not restricted to one pole of the cell. The adjacent connecting segment cells are also labeled, but only at the apical pole. Bar = 25 μm (*Fig. 3*) Detail of cortex, showing sub-brush border labeling in the PCT, marked labeling of all cells in the DCT, a reduced level of labeling in cortical segments of the thick ascending limb of Henle (TAL), and a single, heavily stained intercalated cell in a late portion of the distal convoluted tubule (*arrow*). Bar = 10 μm. (*Fig. 4*) Detail of the cortex, showing apical staining of all cells in a late DCT, with a single intercalated cell that is more heavily stained at the apical pole (*arrow*). An intercalated cell in an adjacent DCT is basally stained. Glomeruli (*G*) are negative. Bar = 10 μm.

Table I. Quantification of H^+ ATPase Antigenic Sites in the Urinary Tubule

Tubule segment/cell type	Gold particles
	per μm membrane
Proximal tubule (convoluted)	6.0±0.6
Proximal tubule (straight)	0.6±0.2*
Thin descending limb (apical)	8.0±0.9
Thin descending limb (basolateral)	5.8±0.5
Thick ascending limb	1.0±0.2*
Distal convoluted tubule	6.5±0.7
Cortical collecting duct	
Type A intercalated cell (apical)	13.6±1.0
Type A intercalated cell (basal)	0.8±0.2*
Type B intercalated cell (apical)	0.6±0.1*
Type B intercalated cell (basal)	8.2±0.6
Type B intercalated cell (lateral)	2.3±0.6
Intercalated cell vesicles (type A cell)	14.4±1.3
Medullary collecting duct	
Intercalated cell (apical)	21.6±1.0
Intercalated cell (basal)	1.0±0.1*
Principal cell (apical)	0.6±0.2*

All results are the mean±SEM of measurements from 10 micrographs. Values are for apical plasma membranes unless otherwise indicated. Figures marked with asterisks are not significantly different from background staining levels measured on sections not exposed to the specific antibody.

In the S2 and S3 segments, no brush border labeling was detected; the qualitative pattern of labeling at the base of the brush border was similar in both segments, but the labeling intensity was much lower than in the convoluted tubule (Table I, Fig. 9).

Thin limbs of Henle. The initial segment of the long, thin descending limb showed marked staining with all antibodies (Fig. 6). The staining was more pronounced at the electron microscope level on K4M sections than at the light microscope level on semithin sections, whereas the staining of all other segments was comparable with both methods. This finding indicates that the initial part of the thin descending limb contains more antigenic sites than other thin limb segments. The labeling of this segment was also unusual in that both apical and basolateral plasma membranes were labeled, although the intensity of labeling was significantly greater ($P < 0.05$) on the apical plasma membrane (Table I, Fig. 6). Other segments of the thin limb were not specifically labeled with any of the antibodies used.

Thick ascending limb and early distal convoluted tubule. In the cortex, the distal convoluted tubule was more heavily stained than the thick ascending limb, and the antigenic sites were again restricted to the apical plasma membrane and to a population of vesicles in the apical cytoplasm (Figs. 2–4, 7). In the medulla, the thick ascending limb of Henle showed a specific, but only weak to moderate staining that was restricted to the apical pole of the epithelial cells (Figs. 3 and 8).

Late distal convoluted tubule, connecting segment and cortical collecting duct. In the early distal tubule, all cells had identical staining, as described above. In later parts of the distal convoluted tubule, intercalated cells, which make their first appearance in this nephron segment, were heavily stained. The remaining late distal convoluted tubule cells had a lighter, apical staining that was distinct from intercalated cells (Figs. 3 and 4). Intercalated cells had three different patterns of labeling: apical, basolateral and diffuse. In Fig. 3, an isolated intercalated cell with heavy apical labeling is shown. The connecting segment (Fig. 2) had many intercalated cells that stained either apically, basolaterally, or diffusely. Included in the category of diffusely stained cells were some cells in which the staining appeared concentrated in both apical and basolateral regions of the cell. As previously described, the number of diffusely stained cells varied considerably among different animals (27). The other less intensely stained cells all had a distinct apical membrane staining, similar to that described for the distal convoluted tubule. The cortical collecting ducts (Figs. 9 and 10) also contained 40% intercalated cells with three different patterns of labeling, but in this segment the remaining cells (the collecting duct principal cells) were stained only weakly or not at all, in contrast to the marked apical staining seen in the non-intercalated cells in prior segments.

At the electron microscope level, the labeling of the distal convoluted tubule and the connecting tubule cells was localized to the apical cytoplasm and some vesicles in the apical cytoplasm, as suggested by immunofluorescence. The principal cells of the cortical collecting duct, however, were virtually unlabeled. In the intercalated cells in all three segments, a heavy labeling was found over parts of the plasma membrane and over a population of vesicles in the cytoplasm. Cells with intense apical staining had very little basolateral staining and probably correspond to type A (proton-secreting) intercalated cells (5, 6, 28). Type B (bicarbonate-secreting) cells had, in contrast, a marked basolateral staining and weak apical staining (Table I). The quantification shows, however, that the intensity of apical labeling of the type A cells is significantly greater than the basolateral staining of type B cells ($P < 0.05$). As we have previously described, the labeling was localized over the specialized stud-coated membrane domains that characterize these cells (2). Due to the preparation conditions required for ultrastructural immunocytochemistry, the membrane-coating studs were not always visible as discrete structures, and often appeared as a dense band on the cytoplasmic face of the membrane (25). In the intercalated cells with basolateral labeling, the staining was concentrated primarily over the basal plasma membrane and was much less intense over the lateral plasma membrane. An abrupt change in labeling intensity delimited these two membrane domains (Fig. 12, Table I).

Medullary collecting duct. In the medullary collecting duct, intercalated cells were heavily labeled, and the adjacent principal cells were weakly labeled (Figs. 8, 11, and Table I). In the outer stripe of the outer medulla, intercalated cells with the varying labeling patterns described in the cortex were found, but the predominant labeling of these outer stripe cells was at the apical pole. In the inner stripe of the outer medulla and in the inner medulla, all intercalated cells had apical labeling. The number of strongly labeled cells fell sharply from almost 45% of the total collecting duct epithelial cells in the inner stripe, to 10% in the initial part of the inner medulla. In the initial third of the inner medullary collecting duct, the number of intercalated cells gradually decreased from 10% to zero, and none were found in the remaining two-thirds of the duct (Fig.

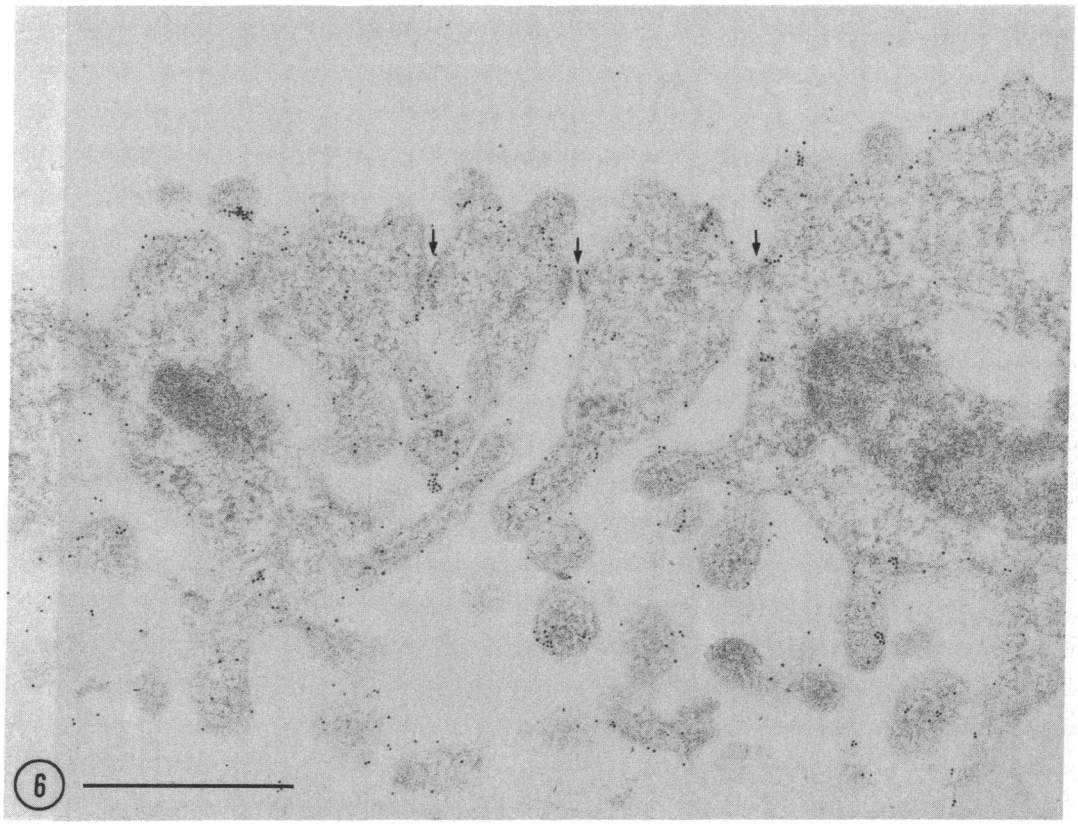

Figure 6. Electron micrograph of part of the initial segment of a thin descending limb of Henle, incubated to reveal antigenic sites with the anti-56-kD subunit antibody, followed by protein A-gold. In this highly interdigitated epithelium (tight junctions are indicated with arrows), both apical and basolateral plasma membrane domains are labeled with the antibody, indicating a lack of polarization of the H^+ATPase in these cells. Bar = 0.5 μm.

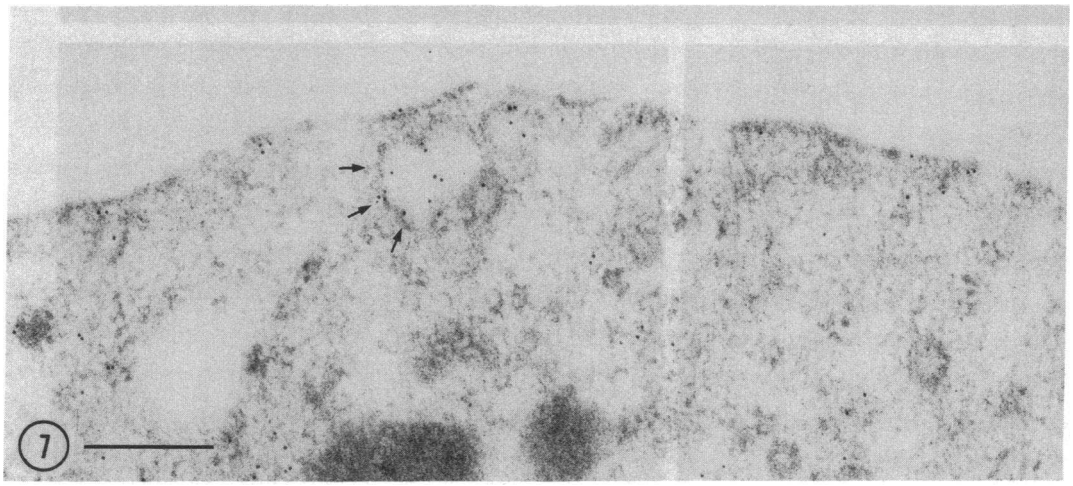

Figure 7. Apical region of a cell from the distal convoluted tubule, incubated with antibodies against the 56-kD subunit of H^+ATPase, and protein A-gold. Label is localized on the cytoplasmic side of the apical membrane, and on some subapical vesicles (*arrows*). Bar = 0.25 μm.

13). By electron microscopy, all intercalated cells in the medulla had an intense gold particle labeling over plasma membrane domains and over the characteristic cytoplasmic vesicles that are found in this cell type. Table I shows that the apical plasma membranes of intercalated cells in this region were the most intensely labeled structures in the entire kidney, and showed a considerably greater staining intensity than membranes from intercalated cells in the cortical collecting duct.

Finally, to demonstrate that all three antibodies above gave the same qualitative pattern of labeling, serial semithin sections of kidney, in which the same cells can be identified throughout, were incubated with our antibodies. Figs. 14–16 show three serial sections of the inner stripe in which H^+ATPase antigenic sites were detected using an immunoperoxidase procedure. It is clear that the same intercalated cells are stained apically with the three different antibodies.

Discussion

Using specific polyclonal antibodies against distinct subunits of a proton-pumping ATPase isolated from bovine kidney medulla, we have localized antigenically similar pump subunits in the rat kidney by light and electron microscopic immunocytochemistry. This study extends our previous observations by showing that the vacuolar-type H^+ATPase is present on the plasma membrane not only of intercalated cells, but also of several other types of renal epithelial cells. In some cells, pumps appeared restricted to certain regions of apical or

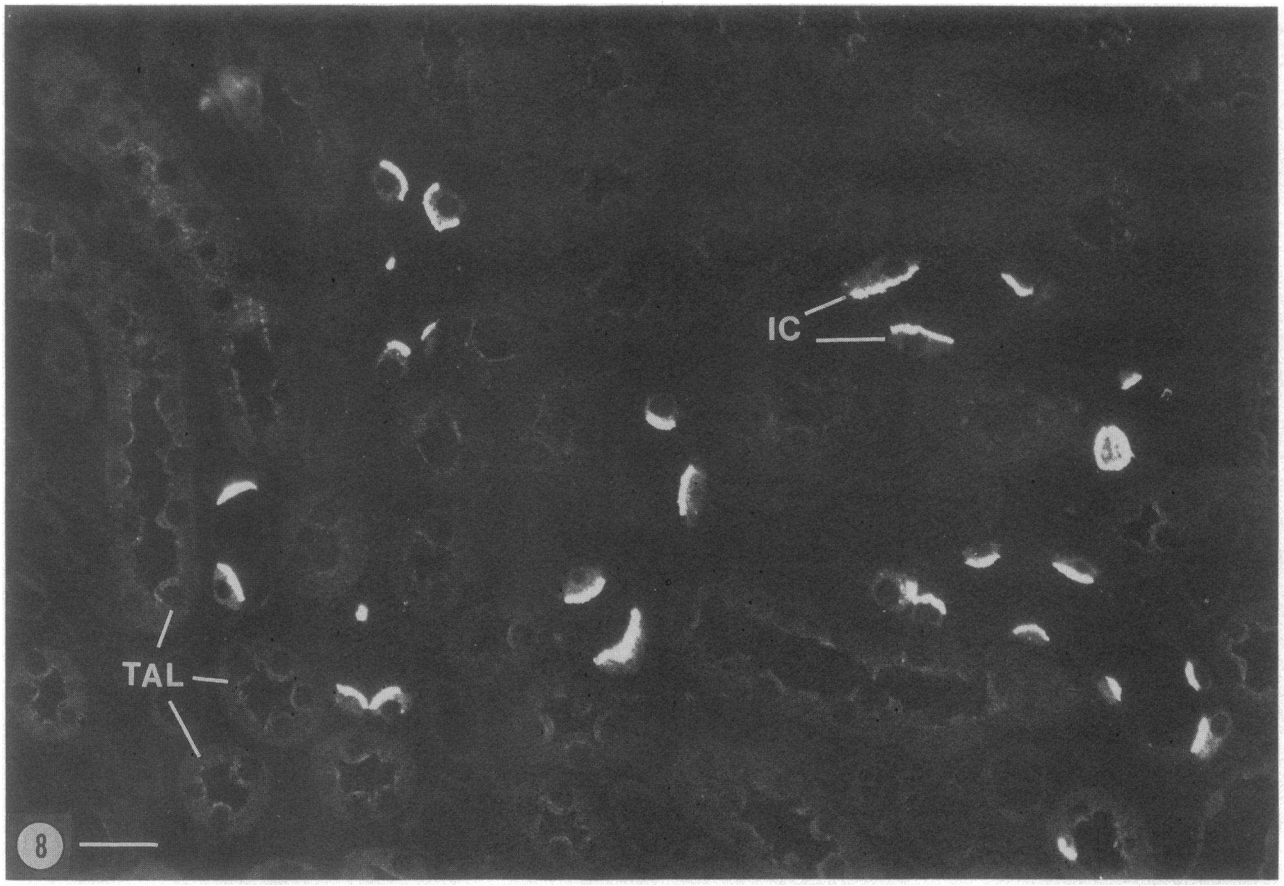
IC
TAL
8

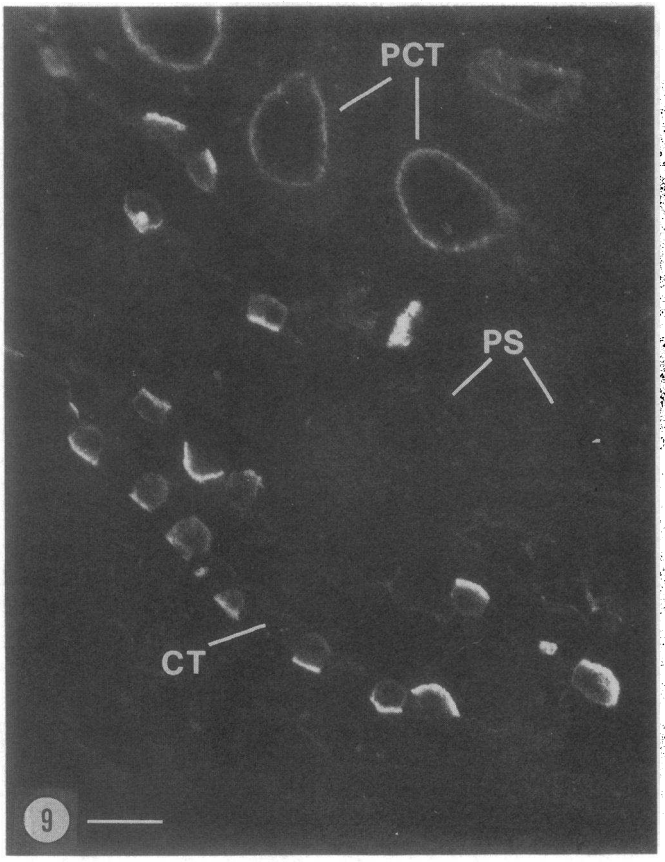
PCT
PS
CT
9


10

basolateral membranes, supporting the concept that renal epithelial cell plasma membranes contain differentiated domains (29, 30). Our findings do not support earlier suggestions that all eucaryotic plasma membrane ion pumps resemble E_1,E_2 type ATPases (17). In the proximal tubule, the localization of proton pumps predominantly in the sub-brush border invaginations and vesicles is direct evidence for the presence of a membrane associated H^+ATPase that is probably involved in hydrogen ion secretion in this nephron segment. The findings agree with recent data showing proton pumping activity in apical vesicle preparations from the proximal tubule (12, 31). Our results also support kinetic models for proximal tubule transport that indicate a requirement for an apical proton pump in order to satisfy the model parameters (13). Studies on isolated, microdissected nephron segments have also described N-ethyl maleimide (NEM)-sensitive ATPase activity in regions where we find immunoreactive sites (10).

The location of the antigenic sites in the proximal tubule appears distinct from the known distribution of clathrin in these cells (25, 26). Coated pits are found in all cell types in the kidney, and no specific labeling of these structures was detectable with our antibodies. This finding is in agreement with some recent data suggesting that proton pumps may be absent from coated pits at the cell surface, and that the coated vesicle proton pump (32, 33) may be found mainly in Golgi-derived coated vesicles (34, 35). However, we cannot exclude the possibility that surface-coated pits could have proton pumps at low density, or that are not cross-reactive with our antibodies. Recently, Sabolic and Burkhardt (36) reported that of the total NEM-sensitive ATPase activity in membranes from kidney cortex, only a small amount was associated with endocytic vesicles. To resolve this question, immunoblotting and immunocytochemical studies on coated vesicles isolated from kidney cortex and medulla will be required.

Studies in which proximal tubule intracellular pH changes have been measured, using fluorescence techniques (11), have suggested that the S3 segment may use proton pumps for pH regulation, consistent with their presence in apical invaginations demonstrated by antibody staining. The straight part of the proximal tubule (S3 segment) had no microvillar staining and had a lower specific labeling than earlier segments, but the significance of these findings is at present unknown.

We found an unexpectedly high level of labeling of epithelial cell plasma membranes in the initial part of the thin descending limb of Henle. The labeling was unusual in that it was present on both apical and basolateral plasma membranes, indicating a lack of polarized insertion of the H^+ATPase in this cell type. The cells in this segment also have an appreciable level of basolateral Na^+, K^+ ATPase activity (37), and an abundance of cytoplasmic carbonic anhydrase (38, 39), suggesting a specialized function that awaits physiological studies for its elucidation. Weak to moderate apical H^+ATPase staining was observed in the thick ascending limb of Henle, a segment that contains substantial carbonic anhydrase (39, 40). The cortical thick ascending limb has ethoxazolamide-sensitive bicarbonate-dependent Na^+ and Cl^- transport, which is thought to represent coupled Na^+/H^+ exchange and Cl^-/HCO_3^- exchange (41, 42). The luminal proton pumps present in this segment might have a role in regulating Na transport or cell pH.

In the cortex, the apical membranes of the distal convoluted tubules showed a stronger labeling than those of the thick ascending limb. These cells also contain abundant carbonic anhydrase activity (39, 40). Under appropriate conditions, the distal convoluted tubule of the rat has substantial rates of H^+ secretion (43). Our results suggest that a proton pump may contribute to H^+ transport or to intracellular pH regulation in this segment, but a role for Na^+/H^+ exchange or other acid/base transporters has not been excluded.

Intercalated cells, which contain the largest amount of carbonic anhydrase of any kidney epithelial cell, first appear in the late part of the distal convoluted tubule (4). These cells have a level of H^+ATPase labeling that is more intense than any other kidney epithelial cell type, supporting the current view that they are the most important distal proton-secreting cells. We have recently shown that the antibodies to the 70-, 56-, and 31-kD subunits of the proton pump all bind to the cytoplasmic domain of the enzyme (2). The rapid-freeze, deep-etch technique has shown that this domain is a 10-nm spherical structure that appears to be composed of multiple subunits, and which is arranged in paracrystalline, hexagonal arrays on the cytoplasmic side of plasma membranes and some cytoplasmic vesicles (2). These H^+ATPase-coated vesicles, which are quite distinct from clathrin-coated vesicles (25), are involved in an exocytotic/endocytotic cycle that delivers proton pumps to, and removes them from the plasma membrane as prevailing systemic acid-base conditions vary (5, 6, 8, 9, 44–48). The different patterns of labeling of intercalated cells in the cortex have been described in a separate report (27). Briefly, we found that some of these cells have a predominantly apical or basolateral staining, while others have a diffuse staining that is not restricted to one pole of the cell. These results provide the first direct evidence of intercalated cells with opposing polarities with respect to an H^+ATPase, as suggested by Schwartz et al. (9), and by Stetson and Steinmetz for analogous carbonic anhydrase-rich cells in the turtle urinary bladder (28). The cells with apical proton pumps are presumably the H^+-secreting cells (type A intercalated cells), whereas those with basolateral staining are the bicarbonate-secreting cells (type B intercalated cells). The presence of cells with differing polarities correlates well with the functional properties of the cortical collecting duct, in which either net bicarbonate reabsorption or secretion may occur, depending on the acid-base status of the animal (49).

Figures 8 and 9. Semithin sections of rat kidney medulla incubated with antibody against the 31-kD subunit of H^+ATPase, followed by goat anti-rabbit FITC. (*Fig. 8*) Semithin section of the inner stripe of the outer medulla of rat kidney stained with the anti-31-kD antibody. Intercalated cells (IC) in this region all have an intense apical fluorescence while adjacent principal cells are negative. In the TAL, all epithelial cells show a weak to moderate apical fluorescence. Bar = 25 μm. (*Fig. 9*) Segment of a cortical collecting duct from a medullary ray, showing the variation in labeling pattern of intercalated cells. Apically stained cells can be seen adjacent to those with basal labeling in a collecting tubule (CT). At the top of the picture, PCT show a marked subapical staining, whereas PST are only weakly stained. Bar = 25 μm.

Figure 10. Detail of part of a cortical collecting duct showing the localization of the 31-kD subunit of the H^+ATPase in the apical or basolateral domain of different intercalated cells. The adjacent principal cells appear unstained. Bar = 10 μm.

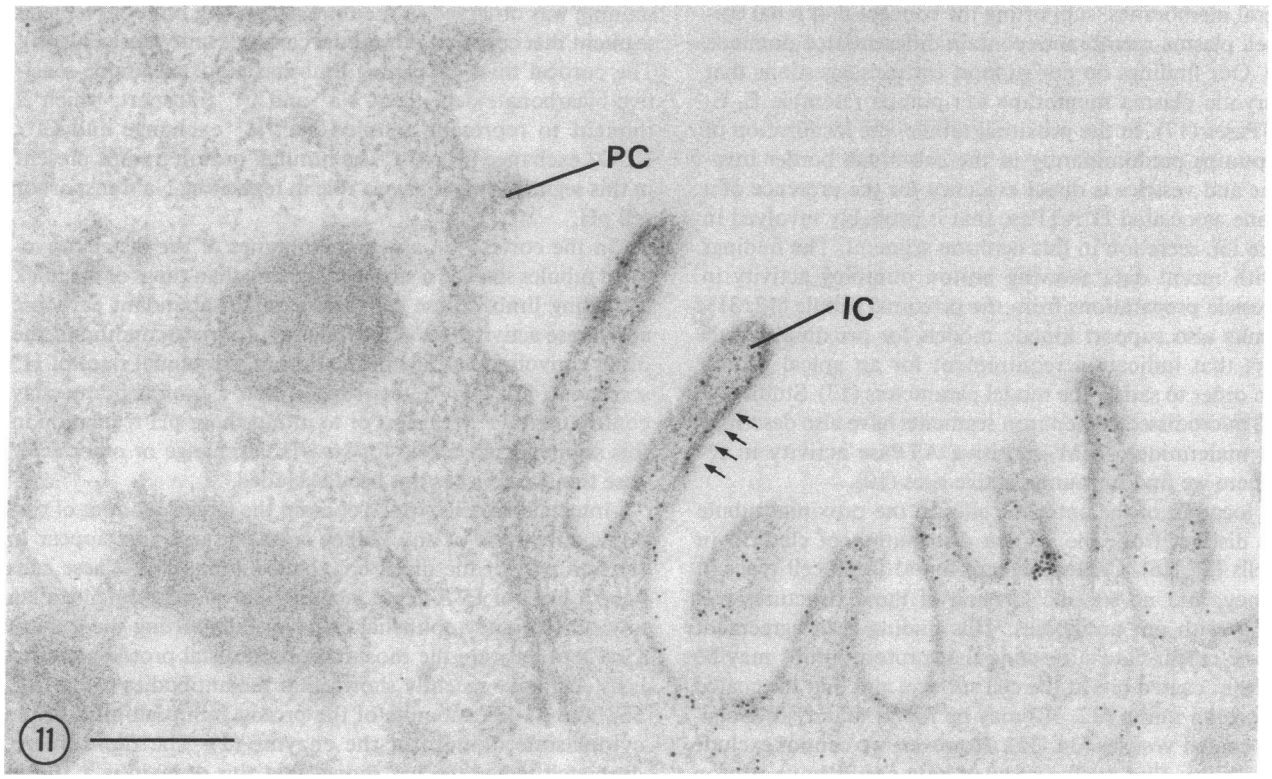

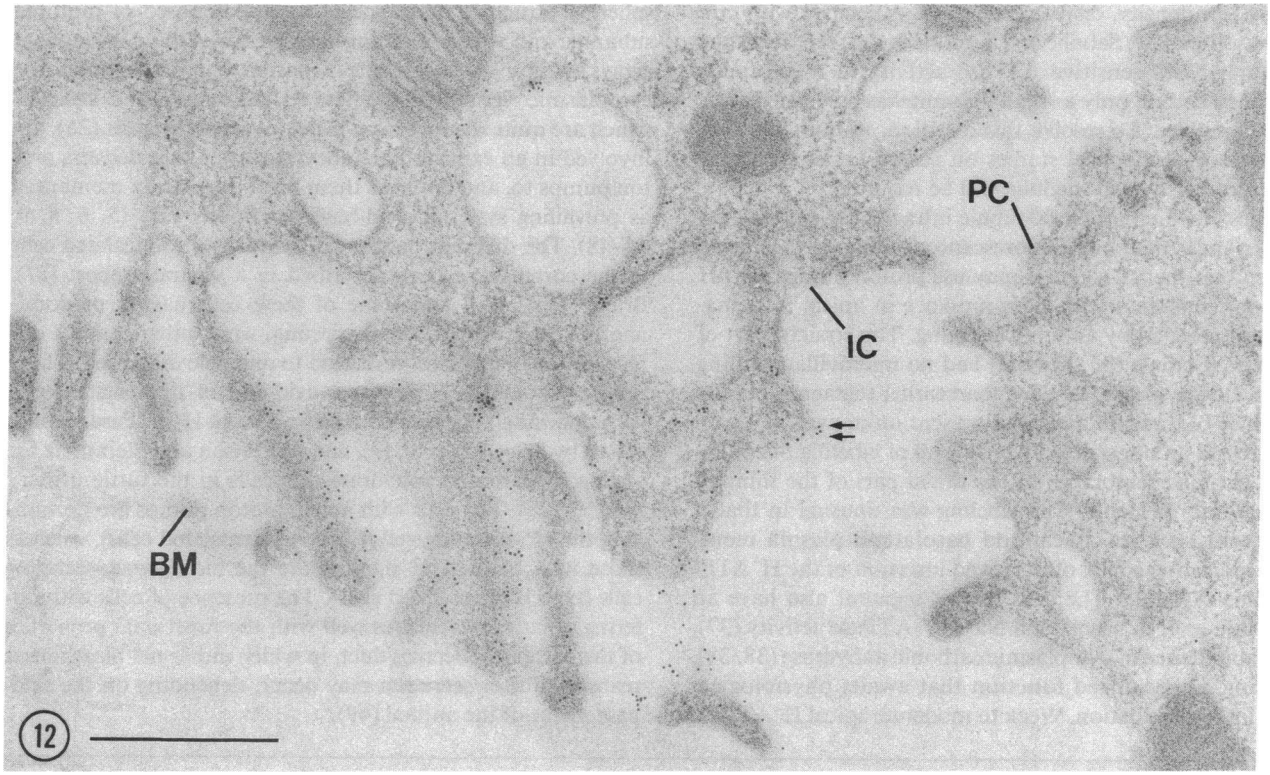

Figure 11. Apical region of a principal cell (PC) and an IC from a medullary collecting duct (*inner stripe*). The intercalated cell is heavily labeled, and the gold particles are mainly located on the cytoplasmic side of the plasma membrane. In perpendicular sections of the membrane, they can be found over a dense submembrane band that corresponds to the H^+ATPase studs (*arrows*), as previously shown (2). The principal cell is unlabeled. Bar = 0.25 μm.

Figure 12. Basal region of a cortical collecting tubule showing an IC adjacent to a PC. This intercalated cell has a heavily labeled basal plasma membrane, but the gold particle labeling shows an abrupt reduction in intensity at the point marked by the arrows. This indicates that H^+ATPase is segregated between basal and lateral plasma membrane domains. The principal cell shows no labeling. BM, basement membrane. Bar = 0.5 μm.

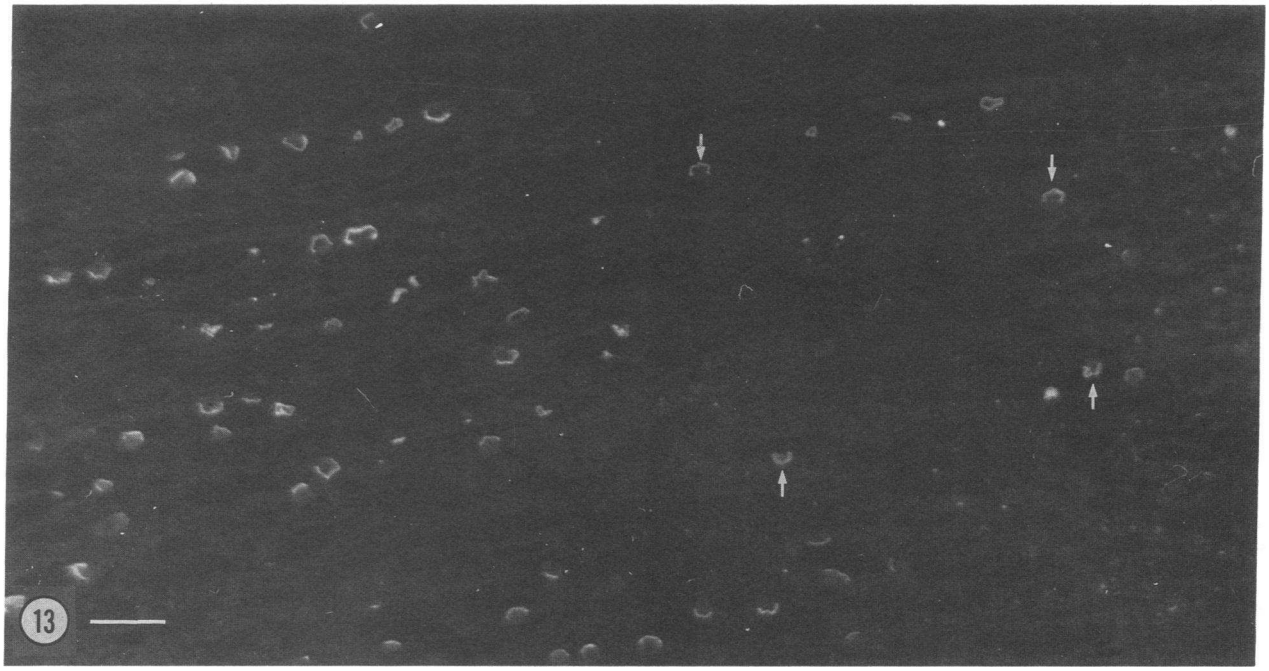

Figure 13. Semithin section of the inner medulla stained with the anti-31-kD subunit antibody. The initial part of the inner medulla, on the left of the picture, shows collecting tubules that contain numerous, positive intercalated cells. In deeper regions of the papilla, to the right of the picture, intercalated cells are much less frequent, and only a few labeled cells can be found (*arrows*). Beyond the middle portion of the papilla, no positive cells were seen. Bar = 35 μm.

The complex H^+ATPase labeling pattern seen in the distal nephron and the initial parts of the collecting duct system reveals heterogeneity of the non-intercalated cells in tubular epithelia that is also reflected by morphological differences (4). Labeling of these segments with antibodies against other antigens such as vitamin D-dependent calcium binding protein (50), Tamm-Horsfall glycoprotein (51), and carbonic anhydrase (38–40), also demonstrates the heterogeneous nature of these cells. Functional studies on the response of isolated, microdissected distal segments to hormones and various physiological stimuli is probably attributable to the presence of different cell types in the various regions examined (52). This complex organization in the cortex contrasts with the medullary collecting ducts which, after the initial portion of the outer stripe, contain only intercalated cells with apical staining and principal cells with poor staining. The solely apical staining and abundance of intercalated cells by immunocytochemistry correlates well with the function of the medullary collecting duct, which has the highest rate of distal H^+ secretion, but does not secrete bicarbonate (53). Our quantitation also showed that intercalated cells in this region are the most heavily labeled cells in the entire kidney. In the inner medulla, heavily stained intercalated cells were detected, with diminishing frequency, along the initial one-third of the ducts, and they were absent from the rest of the papilla. This suggests that intercalated cells may be responsible for at least part of the H^+ secretion measured in this segment (54), rather than the papillary principal cells, although some studies have implicated principal cells in this process (55).

Our results raise a number of questions concerning "morphological markers" that are associated with intercalated cell membranes, and that have been related to the presence of proton pumps on the basis of circumstantial evidence. These markers are (*a*) a cytoplasmic coat of stud-like material that is also found on plasma and vesicle membranes in these cells and (*b*) rod-shaped IMPs seen by freeze-fracture, which are abundant on plasma and vesicle membranes of intercalated cells (56). We have recently demonstrated that the studs are unrelated to clathrin (25), and that they contain subunits of an H^+ATPase (2). Because the studs and the rod-shaped IMPs have not yet been described on all membrane domains in which we detect proton pumps by immunocytochemistry, a more thorough thin section, freeze-fracture and rapid-freezing examination of these membranes will be necessary to determine the relationship between these membrane features.

Finally, our antibodies did not reveal a detectable level of labeling of some cytoplasmic organelles that are known to maintain an acidic internal pH via membrane associated proton pumps. These include endosomes, lysosomes and structures associated with the trans-Golgi apparatus (17). This may be because the number of pumps in the membranes of these organelles is below the detection threshold of immunocytochemistry, or it could be due to a lack of cross-reactivity of these pumps with our antibodies. The latter possibility is unlikely, as the same antibodies show specific binding to a variety of intracellular membrane fractions from bovine kidney and cultured renal epithelial cells (LLCPK1) separated on sucrose and Percoll density gradients (S. Gluck, unpublished observations). In the thick ascending limb and the distal tubule, however, some subapical vesicles possibly representing a class of endosome showed specific labeling. Because the monoclonal antibody initially used to affinity purify the H^+ATPase did detect proton pumps in all acidic compartments in the cultured renal epithelial cells (18), the striking immunocytoche-

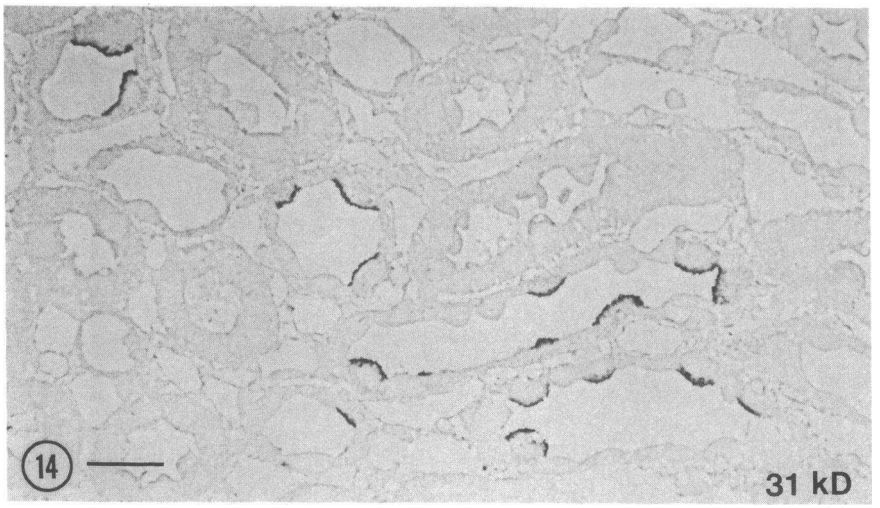

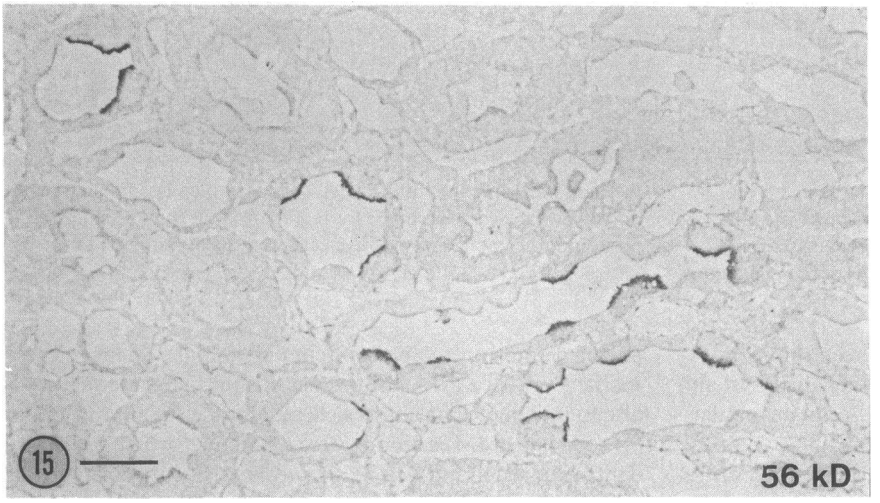

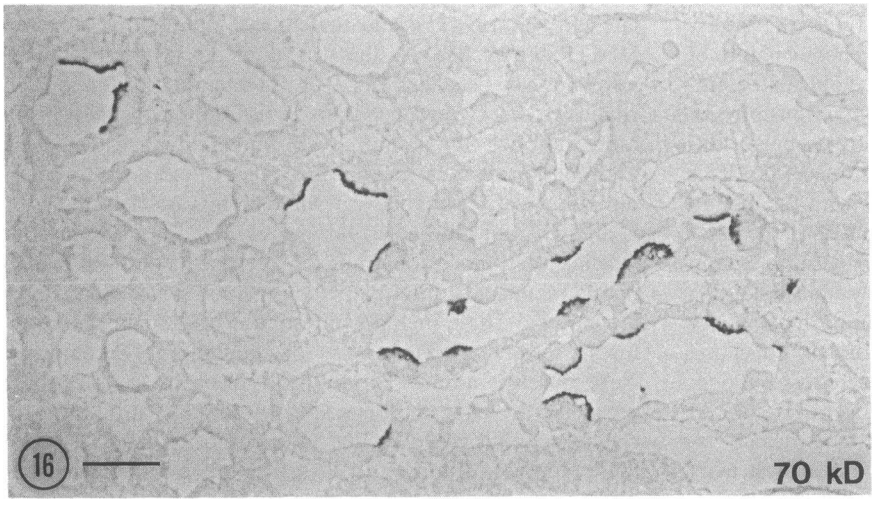

Figures 14–16. Three consecutive semithin sections of the inner stripe of the outermedulla, stained using the ABC-peroxidase procedure with antibodies against the 31-kD subunit of the H^+ATPase (*Fig. 14*), the 56-kD subunit (*Fig. 15*), or the 70-kD subunit (*Fig. 16*). This series of sections shows that all antibodies give a similar pattern of labeling. In particular, the same apically stained intercalated cells can be identified in all three sections. Bar = 30 μm.

mical staining for H^+ATPase in this study appears to reflect high levels of the enzyme in the plasma (and some vesicular) membranes of several types of kidney epithelial cells.

In summary, our data show that vacuolar-type proton pumps reside on the plasma membrane and intracellular vesicles in many cell types along the urinary tubule. They show that at least two types of intercalated cells exist in the cortex, with proton pumps oriented at opposite poles of the cell, and show that proton pumps are in a position to contribute to proximal tubule H^+ transport. The results also indicate a potential role for segments other than the proximal tubule and the collecting duct in acid-base regulation.

Acknowledgments

We thank Joanne Natale for excellent technical help, and Dr. Lee Hamm for comments on the manuscript.

This work was supported by National Institutes of Health grants

DK-38452 and DK-38848, by a National Kidney Foundation Fellowship (S. Hirsch), and by the Searle Scholars Program (S. Gluck). D. Brown is an Established Investigator of the American Heart Association, and was partially supported by a Chugai Fellowship and a grant from the Milton Fund.

References

1. Aronson, P. S. 1983. Mechanisms of active H^+ secretion in the proximal tubule. *Am. J. Physiol.* 245:F647–F659.

2. Brown, D., S. Gluck, and J. Hartwig. 1987. Structure of the novel membrane-coating material in proton-secreting epithelial cells and identification as an H^+ATPase. *J. Cell Biol.* 105:1637–1648.

3. Giebisch, G. 1986. Mechanisms of renal tubule acidification. *Klin. Wochenschr.* 64:853–861.

4. Kaissling, B. 1982. Structural aspects of adaptive changes in renal electrolyte secretion. *Am. J. Physiol.* 243:F211–F226.

5. Madsen, K. M., and C. C. Tisher. 1983. Cellular response to acute respiratory acidosis in rat medullary collecting duct. *Am. J. Physiol.* 245:F670–F678.

6. Madsen, K. M., and C. C. Tisher. 1984. Response of intercalated cells of rat outer medullary collecting duct to chronic metabolic acidosis. *Lab. Invest.* 51:268–276.

7. Richet, G., and J. Hagege. 1975. Dark cells of the distal convoluted tubules and collecting ducts II. Physiological significance. *Fortschr. Zool.* 23:299–306.

8. Schwartz, G. J., and Q. Al-Awqati. 1985. Carbon dioxide causes exocytosis of vesicles containing H^+ pumps in isolated perfused proximal and collecting tubules. *J. Clin. Invest.* 75:1638–1644.

9. Schwartz, G. J., J. Barasch, and Q. Al-Awqati. 1985. Plasticity of functional epithelial polarity. *Nature (Lond.).* 318:368–371.

10. Ait-Mohamed, A. K., S. Marsy, C. Barlet, C. Khadouri, and A. Doucet. 1986. Characterization of N-ethylmaleimide-sensitive proton pump in the rat kidney. *J. Biol. Chem.* 261:12526–12533.

11. Kurtz, I. 1987. Apical Na^+/H^+ antiporter and glycolysis-dependent H^+ATPase regulate intracellular pH in the rabbit S3 proximal tubule. *J. Clin. Invest.* 80:928–935.

12. Sabolic, I., and G. Burckhardt. 1986. Characteristics of the proton pump in renal rat cortical endocytotic vesicles. *Am. J. Physiol.* 250:F817–F826.

13. Verkman, A. S., and R. J. Alpern. 1987. Kinetic transport model for cellular regulation of pH and solute concentration in the renal proximal tubule. *Biophys. J.* 51:533–546.

14. Gluck, S., and Q. Al-Awqati. 1984. An electrogenic proton-translocating adenosine triphosphatase from bovine kidney medulla. *J. Clin. Invest.* 73:1704–1710.

15. Gluck, S., and J. Caldwell. 1987b. Immunoaffinity purification and characterization of H^+ATPase from bovine kidney. *J. Biol. Chem.* 262:15780–15789.

16. Gluck, S., and J. Caldwell. 1988. Proton-translocating ATPase from bovine kidney medulla: partial purification and reconstitution. *Am. J. Physiol.* 254:F71–F79.

17. Mellman, I., R. Fuchs, and A. Helenius. 1986. Acidification of the endocytic and exocytic pathways. *Annu. Rev. Biochem.* 55:663–700.

18. Yurko, M., and S. Gluck. 1987. Production and characterization of a monoclonal antibody to vacuolar H^+ATPase of renal epithelia. *J. Biol. Chem.* 262:15770–15779.

19. Beall, J. A., and G. F. Mitchell. 1986. Identification of a particular antigen from a parasite cDNA library using antibodies affinity purified from selected portions of Western blots. *J. Immunol. Methods.* 86:217–233.

20. McLean, I. W., and P. F. Nakane. 1974. Periodate-lysine paraformaldehyde fixative: a new fixative for immunoelectron microscopy. *J. Histochem. Cytochem.* 22:1077–1083.

21. Altman, L. G., B. G. Schneider, and D. S. Papermaster. 1984. Rapid embedding of tissues in Lowicryl K4M for immunoelectron microscopy. *J. Histochem. Cytochem.* 32:1217–1223.

22. Maxwell, M. H. 1978. Two rapid and simple methods used for the removal of resins from 1 μ thick epoxy sections. *J. Microsc.* 112:253–255.

23. Giloh, H., and S. W. Sedat. 1982. Fluorescence microscopy: reduced photobleaching of rhodamine and fluorescein protein conjugates by n-propyl gallate. *Science (Wash. DC).* 217:1252–1254.

24. Roth, J. 1982. The protein A-gold technique. A qualitative and quantitative approach for antigen localization on thin sections. *In* Techniques in Immunochemistry. G. R. Bullock and P. Petrusz, editors. Academic Press Inc., New York. 107–133.

25. Brown, D., and L. Orci. 1986. The "coat" of kidney intercalated cell tubulovesicles does not contain clathrin. *Am. J. Physiol.* 250:C605–C608.

26. Rodman, J. S., D. Kerjaschki, E. Merisko, and M. G. Farquhar. 1984. Presence of an extensive clathrin coat on the apical plasmalemma of the rat kidney proximal tubule cell. *J. Cell Biol.* 98:1630–1636.

27. Brown, D., S. Hirsch, and S. Gluck. 1988. An H^+ATPase is present in opposite plasma membrane domains in subpopulations of kidney epithelial cells. *Nature (Lond.).* 331:622–624.

28. Stetson, D. L., and P. R. Steinmetz. 1985. a and b types of carbonic anhydrase-rich cells in turtle bladder. *Am. J. Physiol.* 249:F553–F565.

29. Brown, D., and L. Orci. 1988. Junctional complexes and cell polarity in the urinary tubule. *J. Electron Microsc. Tech.* 9:145–170.

30. Kerjaschki, D., L. Noronha-Blob, B. Sacktor, and M. G. Farquhar. 1984. Microdomains of distinctive glycoprotein composition in the kidney proximal tubule brush border. *J. Cell Biol.* 98:1505–1513.

31. Gurich, R. W., and D. G. Warnock. 1986. Electrically neutral Na^+-H^+ exchange in endosomes obtained from rabbit renal cortex. *Am. J. Physiol.* 251:F702–F709.

32. Forgac, M., L. Cantley, B. Wiedenmann, L. Altstiel, and D. Branton. 1983. Clathrin-coated vesicles contain an ATP-dependent proton pump. *Proc. Natl. Acad. Sci. USA.* 80:1300–1303.

33. Stone, D. K., X.-S. Xie, and E. Racker. 1983. An ATP-driven proton pump in clathrin-coated vesicles. *J. Biol. Chem.* 258:4059–4062.

34. Anderson, R. G. W., J. R. Falck, J. L. Goldstein, and M. S. Brown. 1984. Visualization of acidic organelles in intact cells by electron microscopy. *Proc. Natl. Acad. Sci. USA.* 81:4838–4842.

35. Fuchs, R., A. Ellinger, M. Pavelka, M. Peterlik, and I. Mellman. 1987. Endocytic coated vesicles do not exhibit ATP-dependent acidification in vitro. *J. Cell Biol.* 105:91*a*. (Abstr.)

36. Sabolic, I., and G. Burkhardt. 1988. Proton ATPase in rat renal cortical endocytic vesicles. *Biochim. Biophys. Acta.* 937:398–410.

37. Ernst, S. A., and J. H. Schreiber. 1981. Ultrastructural localization of Na^+, K^+ ATPase in rat and rabbit kidney medulla. *J. Cell Biol.* 91:803–813.

38. Brown, D., J. Roth, T. Kumpulainen, and L. Orci. 1983. Immunohistochemical localization of carbonic anhydrase in postnatal and adult rat kidney. *Am. J. Physiol.* 245:F110–F118.

39. Lonnerholm, G., and Y. Ridderstrale. 1980. Intracellular distribution of carbonic anhydrase in the rat kidney. *Kidney Int.* 17:162–174.

40. Dobyan, D. C., and R. E. Bulger. 1982. Renal carbonic anhydrase. *Am. J. Physiol.* 243:F311–F324.

41. Friedman, P. A., and Andreoli, T. E. 1982. CO_2-stimulated NaCl absorption in the mouse renal cortical thick ascending limb of Henle. Evidence for synchronous Na^+/H^+ and Cl^-/HCO_3^- exchange in apical plasma membranes. *J. Gen. Physiol.* 80:683–711.

42. Friedman, P. A. 1986. Bumetanide inhibition of [CO_2 + HCO_3^-]-dependent and independent equivalent electrical flux in renal cortical thick ascending limbs. *J. Pharmacol. Exp. Ther.* 238:407–414.

43. Capasso, G., R. Kinne, G. Malnic, and G. Giebisch. 1986. Renal bicarbonate reabsorption in the rat. 1. Effects of hypokalemia and carbonic anhydrase. *J. Clin. Invest.* 78:1558–1567.

44. Brown, D., P. Weyer, and L. Orci. 1987. Non-clathrin coated vesicles are involved in endocytosis in kidney collecting duct intercalated cells. *Anat. Rec.* 218:237–242.

45. Gluck, S., C. Cannon, and Q. Al-Awqati. 1982. Exocytosis regulates urinary acidification in turtle bladder by rapid insertion of H^+ pumps into the luminal membrane. *Proc. Natl. Acad. Sci. USA.* 79:4327–4331.

46. Steinmetz, P. R. 1986. Cellular organization of urinary acidification. *Am. J. Physiol.* 251:F173–F187.

47. Stetson, D. L., and P. R. Steinmetz. 1983. Role of membrane fusion in CO_2 stimulation of proton secretion by turtle bladder. *Am. J. Physiol.* 245:C113–C120.

48. Stetson, D. L., J. B. Wade, and G. Giebisch. 1980. Morphologic alterations in the rat medullary collecting duct following potassium depletion. *Kidney Int.* 17:45–56.

49. McKinney, T. D., and M. B. Burg. 1977. Bicarbonate transport by rabbit cortical collecting tubules. *J. Clin. Invest.* 60:766–768.

50. Roth, J., D. Brown, and L. Orci. 1982. Localization of vitamin D-dependent calcium-binding protein in mammalian kidney. *Am. J. Physiol.* 243:F243–F252.

51. Hoyer, J. R., S. P. Sisson, and R. L. Vernier. 1979. Tamm-Horsfall glycoprotein: ultrastructural immunoperoxidase localization in rat kidney. *Lab. Invest.* 41:168–173.

52. Morel, F., D. Chabardes, and M. Imbert-Teboul. 1980. Distribution of adenylate cyclase activity in the nephron. *Curr. Top. Membr. Trans.* 13:415–426.

53. Lombard, W. E., J. P. Kokko, and H. R. Jacobson. 1983. Bicarbonate transport in cortical and outer medullary collecting tubules. *Am. J. Physiol.* 244:F289–F296.

54. Graber, M. L., H. H. Bengele, J. H. Schwartz, and E. A. Alexander. 1981. pH and PCO2 profiles of the rat inner medullary collecting duct. *Am. J. Physiol.* 241:F659–F668.

55. Pringent, A., M. Bichara, and M. Paillard. 1985. Hydrogen ion transport in papillary collecting duct of rabbit kidney. *Am. J. Physiol.* 248:C241–C246.

56. Orci, L., F. Humbert, D. Brown, and A. Perrelet. 1981. Membrane ultrastructure in urinary tubules. *Int. Rev. Cytol.* 73:183–242.